

# Independent Co-Option of a Tailed Bacteriophage into a Killing Complex in *Pseudomonas*

Kevin L. Hockett,<sup>a</sup> Tanya Renner,<sup>b,c</sup> David A. Baltrus<sup>a</sup>

School of Plant Sciences, University of Arizona, Tucson, Arizona, USA<sup>a</sup>; Department of Entomology and Center for Insect Science, University of Arizona, Tucson, Arizona, USA<sup>b</sup>; Biology Department, San Diego State University, San Diego, California, USA<sup>c</sup>

**ABSTRACT** Competition between microbes is widespread in nature, especially among those that are closely related. To combat competitors, bacteria have evolved numerous protein-based systems (bacteriocins) that kill strains closely related to the producer. In characterizing the bacteriocin complement and killing spectra for the model strain *Pseudomonas syringae* B728a, we discovered that its activity was not linked to any predicted bacteriocin but is derived from a prophage. Instead of encoding an active prophage, this region encodes a bacteriophage-derived bacteriocin, termed an R-type syringacin. This R-type syringacin is striking in its convergence with the well-studied R-type pyocin of *P. aeruginosa* in both genomic location and molecular function. Genomic alignment, amino acid percent sequence identity, and phylogenetic inference all support a scenario where the R-type syringacin has been co-opted independently of the R-type pyocin. Moreover, the presence of this region is conserved among several other *Pseudomonas* species and thus is likely important for intermicrobial interactions throughout this important genus.

**IMPORTANCE** Evolutionary innovation is often achieved through modification of complexes or processes for alternate purposes, termed co-option. Notable examples include the co-option of a structure functioning in locomotion (bacterial flagellum) to one functioning in protein secretion (type three secretion system). Similar co-options can occur independently in distinct lineages. We discovered a genomic region in the plant pathogen *Pseudomonas syringae* that consists of a fragment of a bacteriophage genome. The fragment encodes only the tail of the bacteriophage, which is lethal toward strains of this species. This structure is similar to a previously described structure produced by the related species *Pseudomonas aeruginosa*. The two structures, however, are not derived from the same evolutionary event. Thus, they represent independent bacteriophage co-options. The co-opted bacteriophage from *P. syringae* is found in the genomes of many other *Pseudomonas* species, suggesting ecological importance across this genus.

Received 17 March 2015 Accepted 17 July 2015 Published 11 August 2015

Citation Hockett KL, Renner T, Baltrus DA. 2015. Independent co-option of a tailed bacteriophage into a killing complex in *Pseudomonas*. mBio 6(4):e00452-15. doi:10.1128/mBio.00452-15.

Editor Steven E. Lindow, University of California, Berkeley

Copyright © 2015 Hockett et al. This is an open-access article distributed under the terms of the [Creative Commons Attribution-Noncommercial-ShareAlike 3.0 Unported license](https://creativecommons.org/licenses/by-nc-sa/4.0/), which permits unrestricted noncommercial use, distribution, and reproduction in any medium, provided the original author and source are credited.

Address correspondence to Kevin L. Hockett, [hockettk@email.arizona.edu](mailto:hockettk@email.arizona.edu).

The genus *Pseudomonas* includes organisms exhibiting diverse ecological strategies and life histories, including human and plant pathogens, plant mutualists, and saprotrophic plant-, soil-, and water-inhabiting organisms (1–7). Many of the environments inhabited by this genus are limited in the available forms of one or several key nutrients (e.g., carbon or nitrogen), which drives intermicrobial competition (8–10). Furthermore, the distribution of nutrients can be spatially limited, which drives competition for colonization of particular anatomical locations (11). Resource competition is a major factor driving the evolution and ecology of microorganisms in many, if not all, environments.

Resource competition between microbes with overlapping niches can resolve in multiple ways, one of which relies on the production of anticompeteritor compounds (i.e., compounds that directly inhibit ecological competitors), including bacteriocins (12, 13). Anticompeteritor strategies are advantageous because they increase resource availability for the producer (14). Bacteriocins are diverse, evolutionarily unrelated peptides, proteins, and protein complexes produced by bacteria that are lethal toward strains

and species closely related to the producer (13, 15). As such, they are recognized as effective anticompeteritor compounds. Indeed, numerous empirical and theoretical studies have demonstrated the adaptive advantage of bacteriocin production (16–19). In addition to basic scientific interest, there is considerable interest in harnessing and modifying bacteriocins as next-generation pathogen control compounds (20–23). Bacteriophage-derived bacteriocins (such as the R- and F-type pyocins) are of particular interest because of their ability to be reprogrammed to specifically target distantly related pathogens with few predicted side-effects (23).

Bacteriocins produced by *Pseudomonas aeruginosa* have been well documented (reviewed in references 15 and 24). *P. aeruginosa* produces three general types of bacteriocins: S-type (soluble) pyocins, which function as single proteins, and R-type (retractile) and F-type (flexible) pyocins, which function as protein complexes and are related to bacteriophage tails of the families *Myoviridae* and *Siphoviridae*, respectively (15, 24). The R-type pyocins can be separated into five groups (R1 to R5) on the basis of targeting

specificity (25, 26), and the atomic structure of the R2 pyocin has recently been described (27). Briefly, R-type pyocins kill cells through dissipation of proton potential, which is achieved by inserting a proton-conducting channel into the bacterial membrane (27, 28).

In contrast to the bacteriocins produced by *P. aeruginosa*, those produced by environmental pseudomonads are less well understood, though this trend is changing (see reference 24 for a recent review), including the description of a phage-derived bacteriocin produced by a plant growth-promoting strain of *Pseudomonas fluorescens* (29). *Pseudomonas syringae* has served as a model species to understand many aspects of plant-microbe interactions, including the microbial ecology of aerial plant surfaces (termed the phyllosphere), as well as the molecular and genomic bases of pathogen-plant interactions (5, 30–33). An important aspect of fitness in the leaf environment for *P. syringae* (and other plant-associated bacteria) is the ability to access and exploit favorable leaf anatomic locations (intercellular grooves, base of glandular trichomes) where water and nutrients are relatively abundant (30, 34). Such scarcity and distribution of resources drive competition among bacteria inhabiting the phyllosphere (8, 35). We expect that bacteriocins play an important role in resolving such resource competition. Indeed, bacteriocins have been predicted among the sequenced genomes of *P. syringae* (reviewed in references 1, 11, 24, and 36 to 38) and some members have been biologically characterized (39).

In this work, we set out to assess the totality of the bacteriocin content of 18 genomes, representing the phylogenetic breadth of *P. syringae*, as well as assess the killing activity spectra of these same strains. In attempting to link the genotype and phenotype of the model strain *P. syringae* B728a, we discovered that its killing activity could not be explained by any predicted bacteriocins. In searching for the source of this killing activity, we discovered a new bacteriophage-derived bacteriocin, or tailocin (in accordance with the terminology used in references 24, 40, and 41). This killing compound represents striking genomic and molecular convergence with the R-type pyocin of *P. aeruginosa* but is independently derived. Additionally, we show that this tailocin is largely conserved throughout *P. syringae* and is present in other related *Pseudomonas* species, though its genomic location is variable. Thus, this killing compound is likely a major mediator of intraspecific interaction across this ecologically important genus.

## RESULTS

***P. syringae* strains commonly exhibit killing activity and harbor diverse predicted bacteriocin loci.** Mitomycin C induction resulted in the production of diverse killing patterns from *P. syringae* pathovars in culture supernatants, as evidenced by the zones of inhibition created by filtered supernatants in a lawn of target strains. The killing activity could be the result of a bactericidal compound or an activated prophage, which are commonly predicted in sequenced *P. syringae* genomes and have been recovered by using this protocol (e.g., 42, 43). Only two strains produced detectable bacteriophage activity (see Fig. S1 in the supplemental material). Though we observed abundant bacteriocin-mediated clearing, we cannot rule out the possibility that bacteriophages were more prevalent but were not detected because their activity was masked by that of a bacteriocin(s) or that induced bacteriophage could not infect the strains included in this study. Additionally, killing activities could result from secondary metabolites.

The genomes of all of the strains were analyzed by several approaches (see Materials and Methods). Class III bacteriocins (>10 kDa) with DNase catalytic domains (colicin E9-like and carocin D-like) were commonly predicted among the strains (see Fig. S2 in the supplemental material). Additional class III bacteriocins predicted among strains include pyocin S3-like (DNase), colicin E3-like (rRNase), colicin D-like (tRNase), colicin M-like (lipid II degrading), and putadecin-like (unknown killing mechanism). In addition to class III bacteriocins, there were several of classes I and II, collectively referred to as ribosomally synthesized and posttranslationally modified peptides (RiPPs), including microcin-like, lasso peptide-like, sactipeptide-like, and linear azol(in)e-containing peptide-like peptides and associated modification and transport proteins. The BAGEL2 and BAGEL3 databases used for bacteriocin prediction contain criteria for all of the major bacteriocin classes, except for bacteriophage-derived bacteriocins, such as the R- and F-type pyocins produced by *P. aeruginosa* (44, 45).

We sought to confirm the genetic basis of the killing activity of *P. syringae* B728a. To this end, we constructed targeted gene deletions for the two predicted colicin-like bacteriocins, Psyr\_0310 and Psyr\_4651 (here referred to as S-type syringacins, in accordance with the naming convention established for *P. syringae* and *P. aeruginosa* [15, 39]). Both S-type syringacins encode putatively DNase-active proteins. Deletion of Psyr\_0310 and Psyr\_4651, individually or in tandem, resulted in no detectable loss of killing activity against any strain targeted by wild-type *P. syringae* B728a (Fig. 1A). This result indicated that the killing activity of *P. syringae* B728a is derived from a source not predicted by genome mining or BLASTp queries using conserved catalytic domains.

***P. syringae* B728a harbors a bacteriophage-derived bacteriocin responsible for its killing activity.** The above results indicated that another locus (or loci) was responsible for the observed killing activity of *P. syringae* B728a. As the killing activity of this strain was more abundant in cultures treated with mitomycin C, we looked for the presence of RecA-mediated autopeptidase regulators, which are known to regulate bacteriocin production in *P. aeruginosa* and are mitomycin C responsive (46). There are nine predicted open reading frames (ORFs) in the *P. syringae* B728a genome that exhibit significant similarity to the consensus sequence of COG1974 (SOS response transcriptional repressors) retrieved from the NCBI Conserved Domain Database (47). One of the predicted RecA-mediated autopeptidases was found associated with previously described prophage region II (48), which is in a genomic location identical to that of the R- and F-type pyocins (specifically, between *trpE* and *trpG*) of *P. aeruginosa* PAO1 (Fig. 2). As both the R- and F-type pyocins are derived from bacteriophages (25), we hypothesized that prophage region II was responsible for the mitomycin C-inducible killing activity. We constructed a series of deletions in both structural and regulatory genes associated with prophage region II (see Fig. S3A and C in the supplemental material). Deletion of a putative transcriptional regulator (Psyr\_4603) encoding a RecA-mediated autopeptidase, as well as the promoter of a divergently transcribed hypothetical protein (Psyr\_4602), resulted in loss of killing activity against all of the strains sensitive to *P. syringae* B728a (Fig. 1A). Because the activities of both Psyr\_4603 and Psyr\_4602 are affected in this deletion strain, we refer to it as  $\Delta R_{reg}$  (indicating the potential deletion of multiple regulatory gene functions). Complementation by the introduction of Psyr\_4603 and Psyr\_4602 (as well as flanking

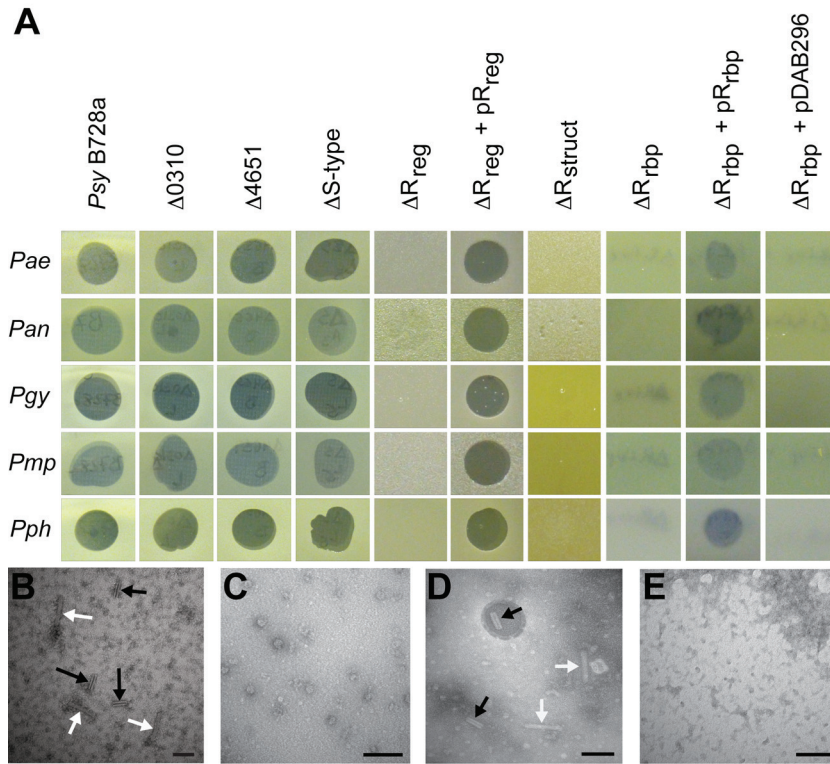


**FIG 1** Clearing activity produced by *P. syringae* B728a and various bacteriocin deletion mutants against selected pathovars (A). Two to 5  $\mu$ l of filter-sterilized, mitomycin C-induced culture supernatant was spotted onto soft agar overlays of the pathovars indicated (rows). *P. syringae* B728a (wild type),  $\Delta$ 0310 (deletion of Psyr\_0310),  $\Delta$ 4651 (deletion of Psyr\_4651),  $\Delta$ S-type (deletion of both Psyr\_0310 and Psyr\_4651),  $\Delta$ R<sub>reg</sub> (deletion of Psyr\_4603 promoter and coding sequence and Psyr\_4602 promoter),  $\Delta$ R<sub>reg</sub> + pR<sub>reg</sub> (R<sub>reg</sub> deletion with both Psyr\_4603 and Psyr\_4602, as well as the surrounding genomic sequence, complemented in *trans* on a replicative vector),  $\Delta$ R<sub>struct</sub> (deletion of Psyr\_4592 through Psyr\_4586, as well as the promoter of Psyr\_4585),  $\Delta$ R<sub>rbp</sub> (deletion of Psyr\_4584 and Psyr\_4585),  $\Delta$ R<sub>rbp</sub> + pR<sub>rbp</sub> (Psyr\_4584 and Psyr\_4585 expressed from a constitutive promoter in pBAV226), and  $\Delta$ R<sub>rbp</sub> + pDAB296 (pBAV266 empty vector). Transmission electron micrographs of mitomycin C-induced cultures of *P. syringae* B728a (B),  $\Delta$ R<sub>reg</sub> (C),  $\Delta$ R<sub>reg</sub> + pR<sub>reg</sub> (D), and  $\Delta$ R<sub>struct</sub> (E). White arrows indicate putative tailocins, and black arrows indicate putative tailocin fragments or contracted tailocins. Bars, 100 nm. Samples were either partially purified by PEG precipitation (B and E) or left unpurified (C and D).

genomic sequences) in *trans* restored the killing activity against all of the strains tested. Deletion of a region encompassing Psyr\_4585 through Psyr\_4592, which includes genes encoding structural components of the baseplate, spike, tail fiber, and tape measure

( $\Delta$ R<sub>struct</sub>), abolished the killing activity against all of the strains. Deletion of the predicted receptor binding protein (Psyr\_4585) and chaperone (Psyr\_4584), which assists in attachment of the receptor binding protein to the baseplate ( $\Delta$ R<sub>rbp</sub>), also abolished

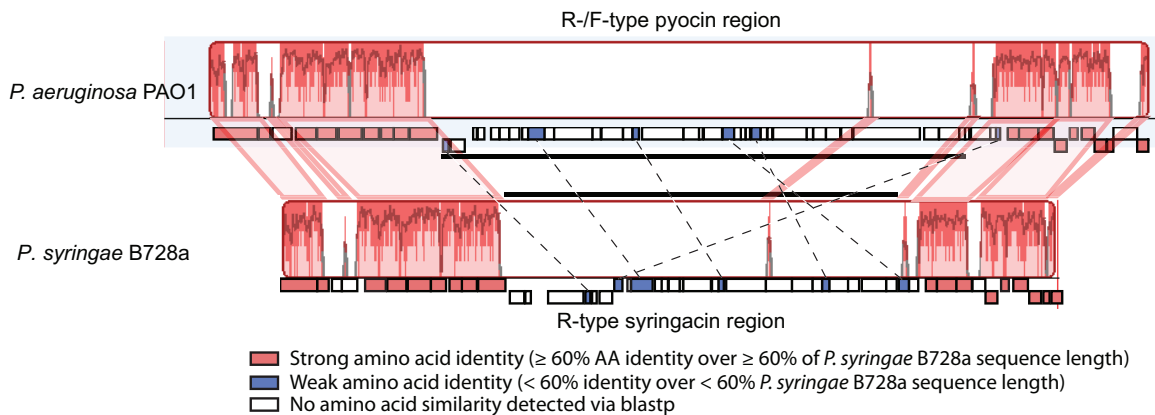


**FIG 2** Comparison of genomic regions flanked by *trpE* and *trpG* between *P. syringae* B728a and *P. aeruginosa* PAO1. Regions between *P. aeruginosa* PAO1 and *P. syringae* B728a connected with pink shading show significant nucleotide identity, as assessed by progressive Mauve. Dashed lines between the respective pyocin and syringacin regions indicate genes that exhibit detectable amino acid (AA) similarity. Dashed lines were omitted between conserved genes in regions of nucleotide identity between *P. aeruginosa* PAO1 and *P. syringae* B728a; however, gene synteny between the two strains is conserved.



the killing activity against all of the strains. Expression of Psyr\_4585/Psyr\_4584 from a constitutive promoter in *trans* restored the killing activity against all of the strains. It should be noted that complementation was possible only for constructs that included an upstream alternative start codon (see Fig. S3B). Additionally, electron microscopy showed the presence of tail-like particles in culture supernatants of the wild-type strain and the complemented regulatory deletion mutant ( $\Delta R_{reg} + R_{reg}$ ) but not in the supernatant of either the  $\Delta R_{reg}$  or the  $\Delta R_{struct}$  deletion mutant (Fig. 1B to E). Taken together, the genetic and phenotypic data convincingly demonstrate that the bacteriophage-derived region is responsible for the intraspecific killing activity of *P. syringae* B728a. In keeping with the *P. aeruginosa* nomenclature, we refer to the killing complex produced by *P. syringae* as an R-type syringacin. We compared the morphology of the R-type syringacin to the recently described R2 pyocin (27), as well as phage SfV (49), the phage most closely related to the R-type syringacin (see below). Precontraction, the R-type syringacin is ~142 nm long by 18 nm wide, which is longer than either the R2 pyocin (100 nm) or the phage SfV tail (105 nm) and approximately equal in width to the R2 pyocin.

**The R-type syringacin of *P. syringae* is derived independently of the R-type pyocin.** Despite the identical genomic locations of the R-type pyocin and R-type syringacin, few genes in these regions exhibit similarity detectable by a BLASTp search with low stringency (*E* value cutoff of  $\leq 10^{-5}$ ; Fig. 2). The R-type syringacin of *P. syringae* B728a was originally described as being related to a Mu-like bacteriophage on the basis of gene content and arrangement (48).

An alignment of the nucleotide sequences surrounding and including the R-type pyocin and syringacin regions demonstrated a high level of identity between the two strains in *trpE* and *trpG* (including genes operonic with these loci) but negligible identity corresponding to the regions encoding the respective tailocins (Fig. 2). This result corresponds to the pattern of amino acid similarity between the ORFs of these regions; those genes located in the *trpE* and *trpG* operons are well conserved between the two strains at the amino acid level, whereas very few genes within the respective bacteriocin regions have detectable amino acid sequence similarity and those that do exhibit relatively little similarity (Fig. 2).

To further confirm that the R-type syringacin from *P. syringae* is derived independently of the R-type pyocin from *P. aeruginosa*, we performed phylogenetic reconstructions by a maximum-likelihood (ML)-based approach for two proteins where amino acid similarity could be detected by BLASTp across *P. syringae* B728a, *P. aeruginosa* PAO1, and phages Mu and P2 by a transitive-homology approach (50) and where all of the proteins were members of the same family. Additionally, by using the same criteria, we included orthologs from sequenced phages belonging to the *Myoviridae* family closely related to either phage Mu or P2 (as described in reference 51), as well as orthologs from sequenced *Pseudomonas* strains. On the basis of the functions predicted or described for the orthologs from P2 and Mu (52, 53), Psyr\_4587 encodes a component of the baseplate and Psyr\_4595 encodes the tail sheath protein. For all of the proteins, there was high bootstrap support (BS; 1,000 replicates) for *P. syringae* B728a orthologs (as well as all of the other *P. syringae* strains examined in this study, except those where the protein was truncated [see below]) being more closely related to those from phage Mu or SfV, whereas

*P. aeruginosa* orthologs were more closely related to those from phage P2 (Fig. 3). Thus, the phylogenetic inference supports the idea that R-type syringacin is derived from an independent bacteriophage (a bacteriophage with a Mu-like tail) rather than the R-type pyocin, although both R-type bacteriocins are located in identical genomic regions. These results are similar to those reported previously, where Mavrodi et al. found the R-type syringacin region (reported by them as genomic island 12) from *P. syringae* B278a exhibited nucleotide sequence similarity to prophage 1 of *Pseudomonas protegens* (*P. fluorescens*) Pf-5, whereas the R-type pyocin of *P. aeruginosa* PAO1 exhibited nucleotide sequence similarity to prophage 3 of Pf-5 (54).

The R-type syringacin appears to be most closely related to phage SfV (rather than phage Mu) on the basis of overall genetic composition (see Table S1 in the supplemental material). The phylogenetic analyses, however, are more ambiguous regarding the relative distance between the R-type syringacin and the two phages (Fig. 3). Importantly, phage SfV harbors an Mu-like tail (55). Though our analyses indicate that the R-type syringacin has been derived independently of the R-type pyocin, comparing the gene content of the R-type syringacin to both phages Mu and SfV demonstrates the loss and retention of genes similar to those described for the R-type pyocin. Specifically, the R-type syringacin lacks all of the genes corresponding to replication functions and head morphogenesis in phages Mu or SfV. The retained genes correspond only to tail morphogenesis or regulation of either phage Mu or SfV (Fig. 4; see Table S1). This pattern of gene retention mirrors that of the R-type pyocin compared to phage P2 (25). These results indicate convergent bacteriophage co-option at both the genomic and phenotypic levels.

In contrast to genes encoding components of the phage tail, prediction of genes associated with lysis functions was more complicated. No gene within this region displays sequence similarity to any described holin. There are two predicted chitinases (Psyr\_4583 and Psyr\_4600) within this region, which may harbor peptidoglycan-degrading (endolysin) activity, as chitinases have been shown to exhibit such activity (56, 57), and chitinase domains have been predicted within phage genomes previously (58, 59). It is important to note that Psyr\_4583 has been annotated as a class I chitinase (family 19 glycoside hydrolase); however, this sequence does not contain typical class I chitinase domains and signatures, such as a chitin recognition or binding domain signature (PS00026), a proline-rich hinge, or a catalytic domain with a chitinase 19\_1 signature (PS00773) and a chitinase 19\_2 signature (PS00774) (60). On the basis of sequence similarities to lysozyme, we suspect that Psyr\_4583 is a family 18 glycoside hydrolase. We were able to predict one spanin-encoding gene (Psyr\_4582). Thus, there is an incomplete accounting of all of the required lysis functions within this region. This may be because lysis functions are provided by genes in this region that lack sequence similarity to known lysis genes or because lysis functions are provided in *trans* from prophage region I, which harbors an active prophage (K. L. Hockett and D. A. Baltrus, unpublished results).

**The R-type syringacin is conserved across *Pseudomonas*.** A previous report (54) demonstrated nucleotide conservation between prophage 1 of *P. fluorescens* Pf-5 (recently renamed *P. protegens* Pf-5; 61) and the R-type syringacin (referred to as genomic island 12). We confirmed the homology of these regions by comparing the amino acid sequence conservation and synteny of genes in their respective regions (data not shown). There is significant

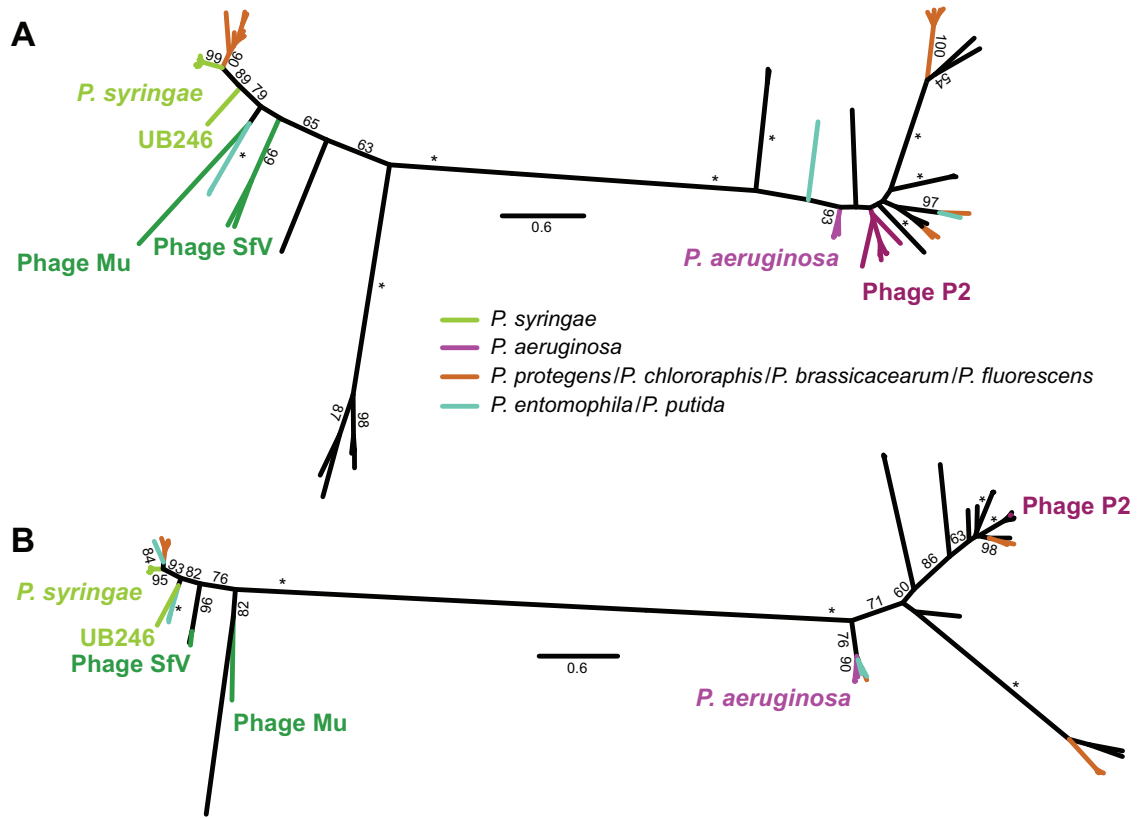


**FIG 3** Best-scoring trees from RAXML ML searches with bootstrap support (BS) values (1,000 replicates). (A) Psyr\_4587 (*P. syringae* B728a), PA0618 (*P. aeruginosa* PAO1), gp47 (Mu), gpJ (P2), and related *Pseudomonas* and *Myoviridae* homologs. (B) Psyr\_4595 (*P. syringae* B728a), PA0622 (*P. aeruginosa* PAO1), gpL (Mu), gpFI (P2), and related *Pseudomonas* and *Myoviridae* homologs. BS values of 100 are denoted by asterisks, whereas BS values of >50 but <100 are reported along the branches. Branches are color coded on the basis of species designations as follows: light green, *P. syringae*; magenta, *P. aeruginosa*; orange, *P. protegens*, *P. chlororaphis*, *P. brassicacearum*, and *P. fluorescens*; cyan, *P. entomophila* and *P. putida*. Branches corresponding to phages Mu and P2 are dark green and red, respectively.

similarity at the amino acid level between most of the tail structural genes. Additionally, the order of genes is syntenic between the two organisms. The most dissimilar genes in the two regions are those encoding the receptor binding proteins (also referred to as the tail fibers), Psyr\_4585 and PFL\_1226, exhibiting only 66% amino acid similarity over 8.6% of the length of Psyr\_4585). This result is not unexpected, however, given this protein's role in host recognition and that it is highly divergent between related bacteriophages, as well as between R-type pyocins encoded among strains of *P. aeruginosa* (24, 62). Our results, in conjunction with those previously reported, indicate that prophage I of *P. protegens*

Pf-5 is homologous to the R-type syringacin and thus likely encodes a killing compound within this organism.

As previously shown (54, 63) prophage I of *P. protegens* Pf-5 is similar to prophage regions found in closely related *P. fluorescens* strains, as well as other pseudomonads. These previous results indicate that R-type syringacin-like elements exist in *P. chlororaphis* 30-84 and O6 and *P. fluorescens* PfO-1. Additionally, sequence clusters resembling the R-type pyocin have also been reported in the genomes of *Pseudomonas* species other than *P. aeruginosa* (24). Thus, we were interested in the distributions of the pyocin-like and syringacin-like tailocins across *Pseudomonas*.

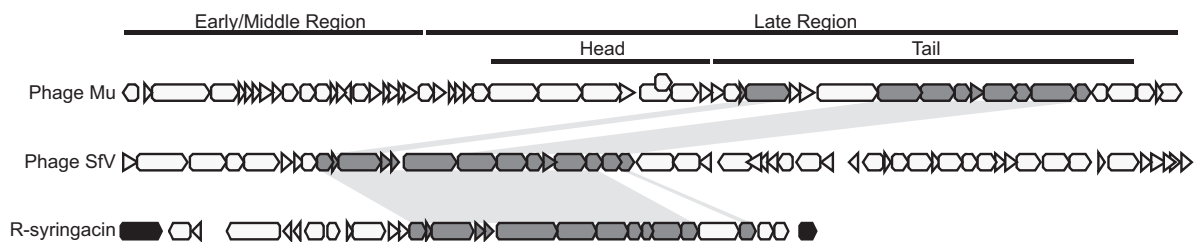


**FIG 4** Comparison of gene contents of the R-type syringacin region and the bacteriophage Mu and SfV genomes. Genes exhibiting amino acid similarity detectable by BLASTp are dark gray. *trpE* (leftmost) and *trpG* (rightmost) are black. Designations of phage Mu gene categories (early, middle, late, head, and tail) are taken from reference 52.

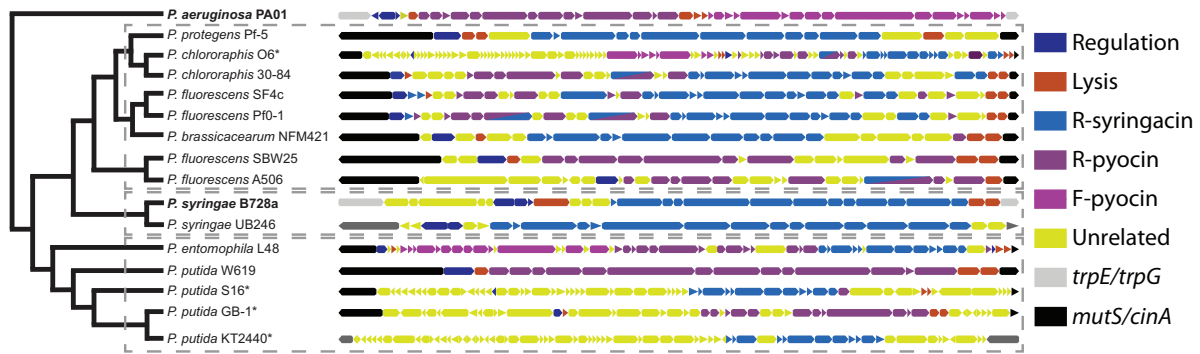


**FIG 5** Comparison of tailocin-related regions across selected *Pseudomonas* species. Phylogeny was constructed with REALPHY (80). Genes are colored as follows. Dark blue and orange indicate amino acid sequence similarity to regulatory or lysis genes, respectively, of either the R- or F-pyocin of *P. aeruginosa* or the R-syringacin of *P. syringae*. Light blue genes are those bearing amino acid sequence similarity to the structural genes of the R-syringacin (P syr\_4584 to P syr\_4597). Dark and light purple genes are those bearing amino acid similarity to the structural genes of either the R-pyocin (PA0614 to PA0628) or the F-pyocin (PA0632 to PA0648), respectively. Yellow indicates genes not bearing amino acid similarity to structural, regulatory, or lysis genes associated with either the *P. syringae* or the *P. aeruginosa* tailocin. Flanking light gray genes are *trpE* and *trpG*. Flanking black genes are *mutS* and *cinA*. Flanking dark gray genes are variable flanking genes. Note that genes within a genome are scaled relative to each other, but because of the difference in gene content among the tailocin regions of different strains, the gene sizes are not scaled among the genomes. Asterisks indicate genomic regions that harbor non-tail phage genes.

Using structural, regulatory, and lytic genes from the pyocin and syringacin regions, we found a broad distribution of R-syringacin-like, R-pyocin-like, and (to a lesser extent) F-pyocin-like regions across *Pseudomonas* (Fig. 5). In the majority of the strains, the tailocin-like regions are located in an alternate genomic location (flanked by *mutS* and *cinA*), which has previously been noted (24, 63). For two strains, *P. syringae* UB246 and *P. putida* KT2440, the R-syringacin clusters are found in genomic locations different from those of *trpE/trpG* and *mutS/cinA*. Interestingly, several of the strains harbored both syringacin-like and pyocin-like clusters, including *P. chlororaphis* O6 and 30-84, *P. fluorescens* SF4c and Pf0-1, and *P. entomophila* L48. Finally, the tailocin-like clusters of four strains (*P. chlororaphis* O6 and *P. putida* S16, GB-1, and KT2440) were collocated with additional phage genes encoding

non-tail morphogenesis functions, indicating that these regions may be prophages rather than tailocins.

The R-type syringacin region is conserved among *P. syringae* strains (Fig. 3), including *P. syringae* UB246, an early diverging strain of this species (7, 64). Within the P syr\_4587 and P syr\_4595 gene phylogenies, however, strain UB246 does not cluster with the other *P. syringae* strains (Fig. 3).

**Naming of genes associated with the R-type syringacin.** As we have described the function and a portion of the molecular determinants of a bacteriophage-derived bacteriocin in *P. syringae* B728a, we have named genes associated with this complex *rtsA* to *-T* for R-type syringacin (Fig. 6). Our aim in naming these genes is twofold. First, providing uniform nomenclature for this structure reflects its specialization as a killing complex, and not simply a

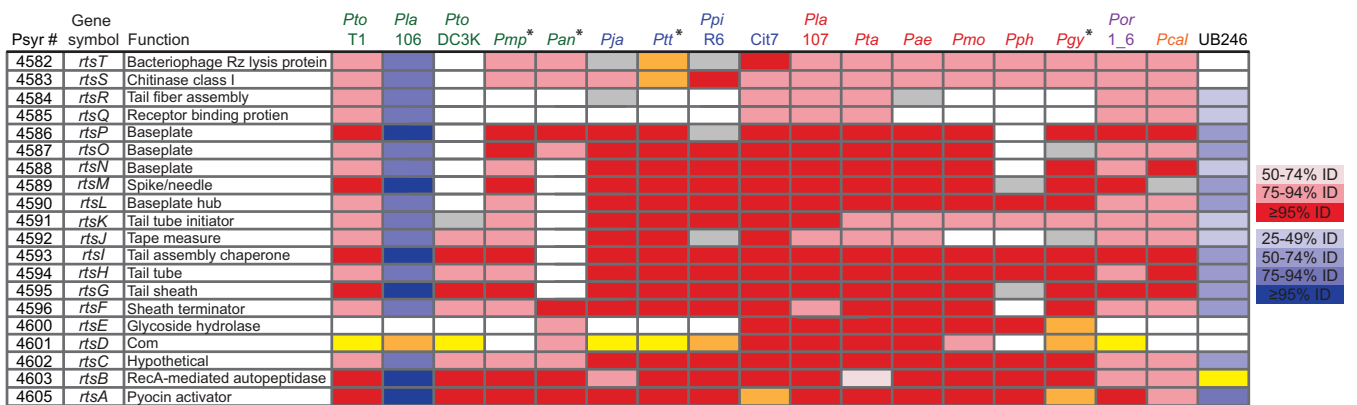


**FIG 6** Conservation of R-type syringacin across *P. syringae*. Cells in shades of red indicate genes with the noted percent amino acid sequence identity (ID) to the *P. syringae* B728a homolog that are syntenic to the R-type syringacin in *P. syringae* B728a. Gray cells indicate genes that are syntenic to the R-type syringacin of *P. syringae* B728a and exhibit amino acid similarity detectable by BLASTp but have less than 60% query coverage (potentially indicating that the gene is truncated compared to the ortholog in *P. syringae* B728a). Yellow cells indicate genes that exhibit significant amino acid identity ( $\geq 80\%$ ) to the *P. syringae* B728a gene indicated; however, the genes are present in a nonsyntenic region of the genome indicated. Orange cells indicate genes that exhibit significant amino acid identity ( $\geq 80\%$ ) to the *P. syringae* B728a gene indicated; however, their locations within their respective genomes cannot be determined. Blue cells (UB246, Pla 106) indicate genes that exhibit detectable similarity to those indicated in *P. syringae* B728a; additionally, the genes are present in the same order as those in the R-type syringacin but are located in a different genomic region (not flanked by *trpE* and *trpG*; UB246) or are on a contig not linked to either *trpE* or *trpG* (ambiguous genomic location; Pla 106). Functional assignments are based on amino acid sequence similarity to phage Mu or SfV (*rtsD*, *rtsF*-*rtsP*, *rtsR*), synteny with described genes from phage (*rtsQ*), or gene annotation at the IMG website (*rtsA* to *rtsC*, *rtsE*, *rtsS*, *rtsT*). Asterisks indicate that R-syringacin regions from the strains indicated are found on two separate contigs, each harboring either *trpE* or *trpG*.

degenerate prophage. Second, we hope that this nomenclature will aid researchers to distinguish this region from the R-type pyocin, especially when discussing homologous tailocins produced by *Pseudomonas* species other than *P. syringae* and *P. aeruginosa* (e.g., *P. fluorescens* and *P. putida*).

## DISCUSSION

Given the diversity and distribution of bacteriocins across *P. syringae*, as well as related pseudomonads (24, 38, 63), it is highly likely that these systems mediate ecological and evolutionary interactions between organisms in the plant environment and beyond. Indeed, that Mavrodi et al. found the region harboring the R-type bacteriocin present in *P. fluorescens* strain Q8r1-96 but absent from strain Q2-87, which is less competent at colonizing the wheat rhizosphere, indicates that this region could affect root colonization (54, 65). Additionally, Garrett et al. found a general trend where *P. syringae* isolates recovered from citrus tended to produce bacteriocins active against isolates recovered from pears and vice versa (66). Direct demonstration of the benefit of bacteriocins in plant colonization is still lacking and thus is an area ripe for future investigation.

Previous work by Fischer et al. demonstrated the presence of a bacteriophage tail-like bacteriocin produced by *P. fluorescens* SF4c that killed related *P. fluorescens* strains (29). Our comparison indicates that the tailocin region of this strain contains components related to both the R-type pyocin and the R-type syringacin (Fig. 5), potentially representing a hybrid tailocin. Thus, it appears that tailocins are more common and widespread throughout *Pseudomonas* than previously recognized. Indeed, previous studies of bacteriocins of *P. syringae* strains indicated the production of high-molecular-weight bacteriocins (synonymous with tailocins) (67), including reports of phage-like particles, such as syringacin 4-A (43). To our knowledge, however, research from this era did not characterize the genetic basis of these proteins. That our genomic predictions initially identified only low-molecular-weight bacteriocins but not the R-type syringacin likely reflects the relative difficulty in predicting the latter compared to the former. Indeed, although the R-type syringacin and R-type pyocin are functionally similar and located in the same region of their respective genomes, the fact that they display negligible gene nucleotide or amino acid identity precludes prediction based on sequence similarity. Thus, *de novo* prediction of tailocins from a genomic sequence is a difficult task, unless the tailocin is closely related to one that has been previously characterized.

Both this and previous work found R-type syringacin-like regions throughout *Pseudomonas* intragenic cluster II (68), including *P. protegens*, *P. chlororaphis*, *P. fluorescens*, *P. brassicacearum*, *P. putida*, *P. entomophila*, and *P. syringae* (54, 63). The R-type syringacin is widely distributed throughout this group of related pseudomonads with a complex evolutionary history. This region appears after the divergence of *P. aeruginosa* from the other species. In *P. syringae*, the R-type region is found nearly exclusively between *trpE* and *trpG*, the only exception being strain UB246, an early diverging member of *P. syringae* sensu lato (64), indicating a single introduction into this species. Interestingly, several strains, including *P. chlororaphis* O6 and 30-84, *P. fluorescens* SF4c and Pf0-1, and *P. entomophila* L48, harbor genes resembling components of both the R-type pyocin and R-type syringacin, potentially indicating recombination between the two tailocins. Additionally, both tailocin clusters (syringacin and pyocin) are colocalized with

genes involved in phage replication and head morphogenesis in *P. chlororaphis* O6 and *P. putida* S16, GB-1, and KT2440. These results indicate that such regions are more likely prophages rather than tailocins. Indeed, this region of *P. putida* KT2440 has previously been described as a prophage region with a phage Mu-like tail gene operon and a phage Sfi21-like head gene cluster (69, 70). To our knowledge, however, there has been no published description of infective bacteriophage being produced from any of these regions.

The results presented above clearly demonstrate the co-option of a retractile-type bacteriophage into a retractile-type bacteriocin independent of the R-type pyocin of *P. aeruginosa*. At the DNA level, there is a high degree of identity between *P. aeruginosa* and *P. syringae* in *trpE* and *trpG* (and the surrounding genomic regions) that is absent from the corresponding bacteriocin regions. Additionally, amino acid sequence similarity between the genes associated with each bacteriocin is scant and likely reflects similarity based on conserved function, as both bacteriocins are derived from related bacteriophages (both in the *Myoviridae* family) (53). Finally, the phylogenetic reconstruction based on two structural proteins provides strong support for separating all of the *P. syringae* R-type syringacin sequences into a clade with bacteriophages Mu and SfV, whereas the *P. aeruginosa* R-type pyocin sequences were present in a clade with bacteriophage P2, indicating that they are independently derived.

The convergence between these two bacteriocins is striking at both the genomic and molecular levels. Given that the R-type syringacin region is located in at least three (possibly four) distinct genomic locations across all of the strains included in this study, this region has likely mobilized in certain lineages following co-option. However, we cannot conclusively determine which location was the ancestral location where the prophage was originally co-opted to a tailocin. The distinct locations include the region between *trpE* and *trpG* (*P. syringae* pathovars), the region between *mutS* and *cinA* (*P. fluorescens* and closely related strains, *P. entomophila*, and *P. putida* S16), and undefined regions of *P. syringae* UB246 and *P. putida* KT2440. It is particularly interesting that the tailocin of *P. syringae* pathovars and the tailocin of *P. aeruginosa* are found in identical genomic locations, despite being derived independently. It is unclear what features favor mobilization or integration into this region. In any event, the convergence of these events implies that there is selective pressure for genetic integration at this locus in *Pseudomonas*. At the molecular level, the profiles of gene retention and loss of the R-type pyocin and R-type syringacin are similar. Genes encoding functions related to replication, capsid morphogenesis, and DNA packaging have been lost in the tailocins, with only genes encoding functions related to bacteriophage tail morphogenesis being retained. Again, these results point to strong selective pressure favoring the co-option of bacteriophages into killing complexes. This work contributes to the body of research demonstrating the adaptive potential provided by bacteriophages to their bacterial hosts (41, 71).

## MATERIALS AND METHODS

**Plasmids, primers, bacterial isolates, and growth conditions.** For the bacterial strains and plasmids used in this study, see Table S2 in the supplemental material; for the primers used, see Table S3. *P. syringae* was routinely grown at 27°C on King's medium B (KB) (72). *Escherichia coli* was routinely grown in lysogeny broth (73) at 37°C. When appropriate, the growth medium was supplemented with tetracycline at 10 µg/ml,



kanamycin at 50  $\mu\text{g/ml}$ , gentamicin at 25  $\mu\text{g/ml}$ , rifampin at 50  $\mu\text{g/ml}$ , nitrofurantoin (NFT) at 50  $\mu\text{g/ml}$ , or 5% (wt/vol) sucrose.

**Deletion and complementation of bacteriocin loci.** Colicin-like and R-type-associated syringacin loci were deleted by an overlap-extension approach similar to that described in reference 74. Approximately 0.8- to 1.0-kbp sequences flanking targeted genes were amplified with *Pfx* polymerase (a proofreading polymerase). Amplified fragments were separated and purified from an agarose gel with the QIAquick gel extraction kit (Qiagen, Valencia, CA) and combined into a subsequent PCR mixture. The combined fragments (in the absence of primers) were cycled 10 times, after which BP tailing primers R and F were added and the fragments were subjected to 20 additional cycles. The desired product was isolated from an agarose gel and combined with the entry vector (pDONR207) in a BP Clonase reaction mixture (Invitrogen, Carlsbad, CA). Gentamicin-resistant colonies were screened by PCR to confirm the presence of the desired DNA fragments. Entry vectors confirmed to harbor the correct fragments were combined with the destination vector (pMTN1907) in an LR Clonase reaction mixture (Invitrogen). Following this reaction, kanamycin-resistant colonies were screened by PCR and one colony confirmed to contain the correct fragment was used as the mating donor in a triparental conjugation with *P. syringae* B728a and DAB44 (mating helper). Mating mixtures were plated on KB amended with rifampin, NFT, and tetracycline. Colonies were screened by PCR to harbor the desired construct. A single confirmed isolate was incubated overnight in unamended KB, after which the resultant culture was serially diluted and spotted onto KB amended with sucrose (counterselection against integrated pMTN1907). Single colonies were picked and confirmed to retain the desired deletion by PCR, as well as to be tetracycline sensitive.

For complementation, genes or operons containing their native promoters were amplified with *Pfx*. Amplified fragments were tailed with BP primers in a subsequent PCR and cloned into pDONR207 in a BP Clonase reaction. Isolates confirmed by PCR to contain the desired fragment served as the donor vectors in an LR Clonase reaction with either pJC531 ( $R_{\text{reg}}$ ) or pBAV226 ( $R_{\text{rbp}}$ ) as the destination vector. A plasmid was isolated from one isolate harboring the destination vector confirmed to contain the desired fragment and subsequently electroporated into the appropriate *P. syringae* B728a deletion mutant.

**Assay for killing activity.** Bacteriocin production was induced by treating log-phase broth cultures with mitomycin C (final concentration, 0.5  $\mu\text{g/ml}$ ); they were then allowed to incubate for an additional 12 to 24 h. Supernatant from induced cultures was collected by centrifuging the surviving cells and cell debris and was sterilized either by filtration with a 0.2- $\mu\text{m}$  filter or by adding 5 to 10  $\mu\text{l}$  of chloroform to the culture supernatant. Bacteriocins were occasionally concentrated to increase detectable killing activity by polyethylene glycol (PEG) precipitation. PEG precipitation was performed by adding NaCl (final concentration, 1.0 M) and PEG 8000 (final concentration, 10%) to the culture supernatants and incubating it either in an ice water bath for 1 h or at 4°C overnight. Samples were centrifuged at 16,000  $\times g$  for 30 min at 4°C. Supernatants were decanted, and samples were resuspended in 1/10 or 1/100 of the original volume of buffer (0.01 M Tris, 0.01 M  $\text{MgSO}_4$ , pH 7.0). Residual PEG was removed by two extractions with equal volumes of chloroform. Sterile supernatants (concentrated or not) were tested for killing activity by a standard agar overlay technique (39). Briefly, 100  $\mu\text{l}$  of a log-phase broth tester culture was combined with 3 ml of molten soft agar (0.4% agar) that was mixed by vortexing and poured over a standard KB agar plate (1.5% agar). Plates were allowed to solidify for 30 min to 1 h prior to the spotting of 5  $\mu\text{l}$  of mitomycin C-induced, sterilized supernatant. Plates were allowed to incubate for 24 to 48 h, after which the presence or absence of a clearing zone was determined. To differentiate between bacteriocin-derived clearing and bacteriophage-derived clearing, two tests were performed. First, serial 1/5 dilutions were plated onto the same tester strain. If killing activity was derived from a bacteriophage, dilutions were found where the clearing zone resolved into distinct plaques, whereas if killing activity was derived from a bacteriocin, the clearing zone

did not resolve into distinct plaques. Second, material from clearing zones on a bacterial lawn was transferred with a sterile toothpick to a subsequent agar overlay plate of the same tester strain. Clearing zones derived from bacteriophages yielded clearing on the subsequent plate, whereas clearing zones derived from bacteriocins did not yield subsequent clearing.

**Non-R-type bacteriocin prediction and genomic comparison.** Colicin-like bacteriocins and their associated immunity proteins (IPs) were predicted by using characterized active domains and IPs (provided by D. Walker, University of Glasgow) as BLASTp queries. Additionally, the recently described lectin-like bacteriocin (75) served as a BLASTp query. Pathovar genomes were analyzed by using both the BAGEL2 and BAGEL3 web-based programs (44, 45), which predict a number of different types of bacteriocins, including class I, II, and III bacteriocins. Bacteriocin prediction by BAGEL3 was not performed until after completion of the R-type bacteriocin; thus, the carocin D-like bacteriocin in *P. syringae* B728a was not targeted for deletion, as the source of the killing activity had already been determined.

**R-type bacteriocin prediction and genomic comparison.** The genomic regions of *P. syringae* B728a and *P. aeruginosa* PAO1 immediately surrounding *trpE* and *trpG* were aligned by progressive Mauve (implemented in Geneious v6.1.8, created by Biomatters Ltd., Auckland, New Zealand). Additionally, genes of the two strains were compared at the amino acid level with BLASTp. Hits exhibiting an *E* value of  $\leq 10^{-5}$  were considered significant.

The gene contents of the R-type bacteriocins of *P. syringae* B728a and *P. aeruginosa* PAO1 were compared to those of phages Mu and P2, respectively, at the amino acid level with BLASTp. Hits exhibiting an *E* value of  $\leq 10^{-5}$  were considered significant.

Gene content across the *Pseudomonas* genus was compared by using the Gene Ortholog Neighborhood Viewer (based on the best bidirectional blast hit) at the Integrated Microbial Genomes (IMG) website (<https://img.jgi.doe.gov/>) with both *trpE* and *trpG* as queries. Comparison of R-type syringacin gene content across *P. syringae* pathovars was also performed with the Gene Ortholog Neighborhood Viewer (best bidirectional blast hit). Additionally, genes within the R-type syringacin region that are bacteriophage derived were compared across pathovars by BLASTp.

**Phylogenetic inference of selected genes.** We used a transitive-homology approach (50) to identify structural proteins that exhibited detectable amino acid similarity (and that belong to the same protein family) across the tailocin regions of *P. syringae* B728a and *P. aeruginosa* PAO1, as well as those of phages Mu and P2. Two proteins were recovered, including Psyr\_4587 (corresponding to gp47 [Mu], gpJ [P2], and PA0618 [*P. aeruginosa*]) and Psyr\_4595 (corresponding to gp39 [Mu], gpFI [P2], and PA0622 [*P. aeruginosa*]). By both BLASTp and protein family annotation searches (76), homologs related to Psyr\_4587 (Pfam 04865) and Psyr\_4595 (Pfam 04984) were collected from the genomes of selected *Pseudomonas* strains, as well as bacteriophages closely related to Mu, SfV, or P2 (51). Truncated sequences were excluded from phylogenetic analyses. Hits were aligned with the MAFFT v1.3.3 plug-in (77) in Geneious v6.1.5 (Biomatters Ltd.) with L-INS-I under Blossum30, with a gap open penalty of 1.53 and an offset value of 0.123.

ML heuristic searches were used to estimate phylogenies with RAxML v8.0.9 (78) on the CIPRES Science Gateway under either the WAG + I + G + F (Psyr\_4587, PA0618, gp47, gpJ, and related *Pseudomonas* and *Myoviridae* homologs) or the LG + I + G + F (Psyr\_4595, PA0622, gpL, gpFI, and related *Pseudomonas* and *Myoviridae* homologs) model of evolution, as determined by the Bayesian Information Criterion in ProtTest v3.2 (79). Searches for the phylogenetic reconstruction with the highest likelihood score were performed simultaneously with 1,000 bootstrap replicates by rapid bootstrapping. The resulting phylogenies were edited with FigTree v1.3.1 (<http://tree.bio.ed.ac.uk/software/figtree/>) and Adobe Illustrator.

**Transmission electron microscopy.** Supernatants from mitomycin C-induced cultures of *P. syringae* B728a,  $\Delta R_{\text{reg}}$ , and  $\Delta R_{\text{struct}}$  were concentrated 10-fold by PEG precipitation. Concentrated supernatants were ad-



sorbed onto a carbon filter (300 mesh) and stained with uranyl acetate. Samples were visualized with a Philips CM12 transmission electron microscope at the Arizona Health Sciences Center Imaging Core Facility.

## SUPPLEMENTAL MATERIAL

Supplemental material for this article may be found at <http://mbio.asm.org/lookup/suppl/doi:10.1128/mBio.00452-15/-/DCSupplemental>.

Figure S1, EPS file, 0.9 MB.  
Figure S2, EPS file, 0.6 MB.  
Figure S3, EPS file, 0.7 MB.  
Table S1, DOCX file, 0.1 MB.  
Table S2, DOCX file, 0.2 MB.  
Table S3, DOCX file, 0.1 MB.

## ACKNOWLEDGMENTS

This project was supported by Agriculture and Food Research Initiative competitive grant 2015-67012-22773 from the USDA National Institute of Food and Agriculture to K.L.H. and by startup funds to D.A.B. from the University of Arizona School of Plant Sciences. T.R. acknowledges support from the National Institutes of Health (K12 GM000708).

We thank Erick Karlsrud, Kevin Dougherty, and Rachel Murillo for their help in the generation and testing of the various mutants presented in this work. We thank Daniel Walker for supplying bacteriocin catalytic domain sequences. We thank Tony Day at the Arizona Health Sciences Center Imaging Core Facility for assistance with transmission electron microscopy.

## REFERENCES

- Baltrus DA, Hendry TA, Hockett KL. 2014. Ecological genomics of *Pseudomonas syringae*, p 59–77. In Gross DC, Lichens-Park A, Kole C (ed), *Genomics of plant-associated bacteria*. Springer, Berlin, Germany.
- Lugtenberg BJJ, Bloembergen GV. 2004. Life in the rhizosphere, p 403–430. In Ramos J-L (ed), *Pseudomonas*. Springer, Boston, MA. [http://dx.doi.org/10.1007/978-1-4419-9086-0\\_13](http://dx.doi.org/10.1007/978-1-4419-9086-0_13).
- D'Argenio D. 2004. The pathogenic lifestyle of *Pseudomonas aeruginosa* in model systems of virulence, p 477–503. In Ramos J-L (ed), *Pseudomonas*. Springer, Boston, MA. [http://dx.doi.org/10.1007/978-1-4419-9086-0\\_12](http://dx.doi.org/10.1007/978-1-4419-9086-0_12).
- Sørensen J, Nybroe O. 2004. *Pseudomonas* in the soil environment, p 369–401. In Ramos J-L ed., *Pseudomonas*. Springer, Boston, MA. <http://dx.doi.org/10.1007/978-1-4419-9086-0>.
- Hirano SS, Uppur CD. 2000. Bacteria in the leaf ecosystem with emphasis on *Pseudomonas syringae*—a pathogen, ice nucleus, and epiphyte. *Microbiol Mol Biol Rev* 64:624–653. <http://dx.doi.org/10.1128/MMBR.64.3.624-653.2000>.
- Morris CE, Sands DC, Vinitzer BA, Gloux C, Guilbaud C, Buffière A, Yan S, Dominguez H, Thompson BM. 2008. The life history of the plant pathogen *Pseudomonas syringae* is linked to the water cycle. *ISME J* 2:321–334. <http://dx.doi.org/10.1038/ismej.2007.113>.
- Morris CE, Sands DC, Vanneste JL, Montarry J, Oakley B, Guilbaud C, Gloux C. 2010. Inferring the evolutionary history of the plant pathogen *Pseudomonas syringae* from its biogeography in headwaters of rivers in North America, Europe, and New Zealand. *mBio* 1(3):e00107-10. <http://dx.doi.org/10.1128/mBio.00107-10>.
- Wilson M, Lindow SE. 1994. Coexistence among epiphytic bacterial populations mediated through nutritional resource partitioning. *Appl Environ Microbiol* 60:4468–4477.
- Demoling F, Figueroa D, Bååth E. 2007. Comparison of factors limiting bacterial growth in different soils. *Soil Biol Biochem* 39:2485–2495. <http://dx.doi.org/10.1016/j.soilbio.2007.05.002>.
- Harrison F. 2007. Microbial ecology of the cystic fibrosis lung. *Microbiology* 153:917–923. <http://dx.doi.org/10.1099/mic.0.2006/004077-0>.
- Lugtenberg B, Kamilova F. 2009. Plant-growth-promoting rhizobacteria. *Annu Rev Microbiol* 63:541–556. <http://dx.doi.org/10.1146/annurev.micro.62.081307.162918>.
- Riley MA, Wertz JE. 2002. Bacteriocin diversity: ecological and evolutionary perspectives. *Biochimie* 84:357–364. [http://dx.doi.org/10.1016/S0300-9084\(02\)01421-9](http://dx.doi.org/10.1016/S0300-9084(02)01421-9).
- Riley MA, Wertz JE. 2002. Bacteriocins: evolution, ecology, and application. *Annu Rev Microbiol* 56:117–137. <http://dx.doi.org/10.1146/annurev.micro.56.012302.161024>.
- Kerr B. 2007. The ecological and evolutionary dynamics of model bacteriocin communities, p 111–134. In Riley M, Chavan M (ed), *Bacteriocins*. Springer, Berlin, Germany. [http://dx.doi.org/10.1007/978-3-540-36604-1\\_6](http://dx.doi.org/10.1007/978-3-540-36604-1_6).
- Michel-Briand Y, Baysse C. 2002. The pyocins of *Pseudomonas aeruginosa*. *Biochimie* 84:499–510. [http://dx.doi.org/10.1016/S0300-9084\(02\)01422-0](http://dx.doi.org/10.1016/S0300-9084(02)01422-0).
- Bakkal S, Robinson SM, Ordonez CL, Waltz DA, Riley MA. 2010. Role of bacteriocins in mediating interactions of bacterial isolates taken from cystic fibrosis patients. *Microbiology* 156:2058–2067. <http://dx.doi.org/10.1099/mic.0.036848-0>.
- Heo Y-J, Chung I-Y, Choi KB, Cho Y-H. 2007. R-Type pyocin is required for competitive growth advantage between *Pseudomonas aeruginosa* strains. *J Microbiol Biotechnol* 17:180–185.
- Waite RD, Curtis MA. 2009. *Pseudomonas aeruginosa* PAO1 pyocin production affects population dynamics within mixed-culture biofilms. *J Bacteriol* 191:1349–1354. <http://dx.doi.org/10.1128/JB.01458-08>.
- Kerr B, Riley MA, Feldman MW, Bohannon BJ. 2002. Local dispersal promotes biodiversity in a real-life game of rock-paper-scissors. *Nature* 418:171–174. <http://dx.doi.org/10.1038/nature00823>.
- Gillor O, Kirkup BC, Riley MA. 2004. Colicins and microcins: the next generation antimicrobials. *Adv Appl Microbiol* 54:129–146. [http://dx.doi.org/10.1016/S0065-2164\(04\)54005-4](http://dx.doi.org/10.1016/S0065-2164(04)54005-4).
- Gillor O, Nigro LM, Riley MA. 2005. Genetically engineered bacteriocins and their potential as the next generation of antimicrobials. *Curr Pharm Des* 11:1067–1075. <http://dx.doi.org/10.2174/1381612053381666>.
- Cotter PD, Hill C, Ross RP. 2005. Bacteriocins: developing innate immunity for food. *Nat Rev Microbiol* 3:777–788. <http://dx.doi.org/10.1038/nrmicro1273>.
- Ritchie JM, Greenwich JL, Davis BM, Bronson RT, Gebhart D, Williams SR, Martin D, Scholl D, Waldor MK. 2011. An *Escherichia coli* O157-specific engineered pyocin prevents and ameliorates infection by *E. coli* O157:H7 in an animal model of diarrheal disease. *Antimicrob Agents Chemother* 55:5469–5474. <http://dx.doi.org/10.1128/AAC.05031-11>.
- Ghequire MGK, De Mot R. 2014. Ribosomally encoded antibacterial proteins and peptides from *Pseudomonas*. *FEMS Microbiol Rev* 38:523–568. <http://dx.doi.org/10.1111/1574-6976.12079>.
- Nakayama K, Takashima K, Ishihara H, Shinomiya T, Kageyama M, Kanaya S, Ohnishi M, Murata T, Mori H, Hayashi T. 2000. The R-type pyocin of *Pseudomonas aeruginosa* is related to P2 phage, and the F-type is related to lambda phage. *Mol Microbiol* 38:213–231. <http://dx.doi.org/10.1046/j.1365-2958.2000.02135.x>.
- Williams SR, Gebhart D, Martin DW, Scholl D. 2008. Retargeting R-type pyocins to generate novel bactericidal protein complexes. *Appl Environ Microbiol* 74:3868–3876. <http://dx.doi.org/10.1128/AEM.00141-08>.
- Ge P, Scholl D, Leiman PG, Yu X, Miller JF, Zhou ZH. 2015. Atomic structures of a bactericidal contractile nanotube in its pre- and postcontraction states. *Nat Struct Mol Biol* 22:377–382. <http://dx.doi.org/10.1038/nsmb.2995>.
- Uratani Y, Hoshino T. 1984. Pyocin R1 inhibits active transport in *Pseudomonas aeruginosa* and depolarizes membrane potential. *J Bacteriol* 157:632–636.
- Fischer S, Godino A, Quesada JM, Cordero P, Jofré E, Mori G, Espinosa-Urgel M. 2012. Characterization of a phage-like pyocin from the plant growth-promoting rhizobacterium *Pseudomonas fluorescens* SF4c. *Microbiology* 158:1493–1503. <http://dx.doi.org/10.1099/mic.0.056002-0>.
- Lindow SE, Brandl MT. 2003. Microbiology of the phyllosphere. *Appl Environ Microbiol* 69:1875–1883. <http://dx.doi.org/10.1128/AEM.69.4.1875-1883.2003>.
- O'Brien HE, Thakur S, Guttman DS. 2011. Evolution of plant pathogenesis in *Pseudomonas syringae*: a genomics perspective. *Annu Rev Phytopathol* 49:269–289. <http://dx.doi.org/10.1146/annurev-phyto-072910-095242>.
- Abramovitch RB, Anderson JC, Martin GB. 2006. Bacterial elicitation and evasion of plant innate immunity. *Nat Rev Mol Cell Biol* 7:601–611. <http://dx.doi.org/10.1038/nrm1984>.
- Lindeberg M, Cunnac S, Collmer A. 2009. The evolution of *Pseudomonas syringae* host specificity and type III effector repertoires. *Mol Plant Pathol* 10:767–775. <http://dx.doi.org/10.1111/j.1364-3703.2009.00587.x>.
- Schönherr J. 2006. Characterization of aqueous pores in plant cuticles and permeation of ionic solutes. *J Exp Bot* 57:2471–2491. <http://dx.doi.org/10.1093/jxb/erj217>.

35. Wilson M, Lindow SE. 1994. Ecological similarity and coexistence of epiphytic ice-nucleating (Ice) *Pseudomonas syringae* strains and a non-ice-nucleating (Ice) biological-control agent. *Appl Environ Microbiol* 60: 3128–3137.
36. Grinter R, Milner J, Walker D. 2012. Bacteriocins active against plant pathogenic bacteria. *Biochem Soc Trans* 40:1498–1502. <http://dx.doi.org/10.1042/BST20120206>.
37. Holtsmark I, Eijsink VG, Brurberg MB. 2008. Bacteriocins from plant pathogenic bacteria. *FEMS Microbiol Lett* 280:1–7. <http://dx.doi.org/10.1111/j.1574-6968.2007.01010.x>.
38. Parret A, De Mot. 2002. Bacteria killing their own kind: novel bacteriocins of *Pseudomonas* and other gamma-proteobacteria. *Trends Microbiol* 10:107–112. [http://dx.doi.org/10.1016/S0966-842X\(02\)02307-7](http://dx.doi.org/10.1016/S0966-842X(02)02307-7).
39. Grinter R, Roszak AW, Cogdell RJ, Milner JJ, Walker D. 2012. The crystal structure of the lipid II-degrading bacteriocin syringacin M suggests unexpected evolutionary relationships between colicin M-like bacteriocins. *J Biol Chem* 287:38876–38888. <http://dx.doi.org/10.1074/jbc.M112.400150>.
40. Gill JJ, Young RF. 2011. Therapeutic applications of phage biology: history, practice and recommendations, p 367–410. In Miller AA, Miller PF ed., *Emerging trends in antibacterial discovery: answering the call to arms*. Caister Academic Press, Norfolk, United Kingdom.
41. Touchon M, Bobay L-M, Rocha EP. 2014. The chromosomal accommodation and domestication of mobile genetic elements. *Curr Opin Microbiol* 22:22–29. <http://dx.doi.org/10.1016/j.mib.2014.09.010>.
42. Nordeen RO, Morgan MK, Currier TC. 1983. Isolation and partial characterization of bacteriophages of the phytopathogen *Pseudomonas syringae*. *Appl Environ Microbiol* 45:1890–1898.
43. Haag WL, Vidaver AK. 1974. Purification and characterization of syringacin 4-A, a bacteriocin from *Pseudomonas syringae* 4-A. *Antimicrob Agents Chemother* 6:76–83. <http://dx.doi.org/10.1128/AAC.6.1.76>.
44. de Jong A, van Heel AJ, Kok J, Kuipers OP. 2010. BAGEL2: mining for bacteriocins in genomic data. *Nucleic Acids Res* 38:W647–W651. <http://dx.doi.org/10.1093/nar/gkq365>.
45. van Heel AJ, de Jong A, Montalbán-López M, Kok J, Kuipers OP. 2013. BAGEL3: automated identification of genes encoding bacteriocins and (non-)bactericidal posttranslationally modified peptides. *Nucleic Acids Res* 41:W448–W453. <http://dx.doi.org/10.1093/nar/gkt391>.
46. Matsui H, Sano Y, Ishihara H, Shinomiya T. 1993. Regulation of pyocin genes in *Pseudomonas aeruginosa* by positive (*prtN*) and negative (*prtR*) regulatory genes. *J Bacteriol* 175:1257–1263.
47. Marchler-Bauer A, Zheng C, Chitsaz F, Derbyshire MK, Geer LY, Geer RC, Gonzales NR, Gwadz M, Hurwitz DI, Lanczycki CJ, Lu F, Lu S, Marchler GH, Song JS, Thanki N, Yamashita RA, Zhang D, Bryant SH. 2013. CDD: conserved domains and protein three-dimensional structure. *Nucleic Acids Res* 41:D348–D352. <http://dx.doi.org/10.1093/nar/gks1243>.
48. Feil H, Feil WS, Chain P, Larimer F, DiBartolo G, Copeland A, Lykidis A, Trong S, Nolan M, Goltsman E, Thiel J, Malfatti S, Loper JE, Lapidus A, Detter JC, Land M, Richardson PM, Kyrpides NC, Ivanova N, Lindow SE. 2005. Comparison of the complete genome sequences of *Pseudomonas syringae* pv. *syringae* B728a and pv. *tomato* DC3000. *Proc Natl Acad Sci U S A* 102:11064–11069. <http://dx.doi.org/10.1073/pnas.0504930102>.
49. Allison GE, Angeles DC, Huan PT, Verma NK. 2003. Morphology of temperate bacteriophage SfV and characterisation of the DNA packaging and capsid genes: the structural genes evolved from two different phage families. *Virology* 308:114–127. [http://dx.doi.org/10.1016/S0042-6822\(03\)00198-3](http://dx.doi.org/10.1016/S0042-6822(03)00198-3).
50. Roessler CG, Hall BM, Anderson WJ, Ingram WM, Roberts SA, Montfort WR, Cordes MH. 2008. Transitive homology-guided structural studies lead to discovery of Cro proteins with 40% sequence identity but different folds. *Proc Natl Acad Sci U S A* 105:2343–2348. <http://dx.doi.org/10.1073/pnas.0711589105>.
51. Lavigne R, Darius P, Summer EJ, Seto D, Mahadevan P, Nilsson AS, Ackermann HW, Kropinski AM. 2009. Classification of *Myoviridae* bacteriophages using protein sequence similarity. *BMC Microbiol* 9:224. <http://dx.doi.org/10.1186/1471-2180-9-224>.
52. Morgan GJ, Hatfull GF, Casjens S, Hendrix RW. 2002. Bacteriophage Mu genome sequence: analysis and comparison with Mu-like prophages in *Haemophilus*, *Neisseria* and *Deinococcus*. *J Mol Biol* 317:337–359. <http://dx.doi.org/10.1006/jmbi.2002.5437>.
53. Leiman PG, Shneider MM. 2012. Contractile tail machines of bacteriophages. *Adv Exp Med Biol* 726:93–114. [http://dx.doi.org/10.1007/978-1-4614-0980-9\\_5](http://dx.doi.org/10.1007/978-1-4614-0980-9_5).
54. Mavrodi DV, Loper JE, Paulsen IT, Thomashow LS. 2009. Mobile genetic elements in the genome of the beneficial rhizobacterium *Pseudomonas fluorescens* Pf-5. *BMC Microbiol* 9:8. <http://dx.doi.org/10.1186/1471-2180-9-8>.
55. Allison GE, Angeles D, Tran-Dinh N, Verma NK. 2002. Complete genomic sequence of SfV, a serotype-converting temperate bacteriophage of *Shigella flexneri*. *J Bacteriol* 184:1974–1987. <http://dx.doi.org/10.1128/JB.184.7.1974-1987.2002>.
56. Minic Z, Brown S, De Kouchkovsky Y, Schultze M, Staehelin C. 1998. Purification and characterization of a novel chitinase-lysozyme, of another chitinase, both hydrolysing *Rhizobium meliloti* nod factors, and of a pathogenesis-related protein from *Medicago sativa* roots. *Biochem J* 332: 329–335.
57. Mauch F, Hadwiger LA, Boller T. 1988. Antifungal hydrolases in pea tissue: 1. Purification and characterization of 2 chitinases and 2 beta-1,3-glucanases differentially regulated during development and in response to fungal infection. *Plant Physiol* 87:325–333. <http://dx.doi.org/10.1104/pp.87.2.325>.
58. Resch G, Kulik EM, Dietrich FS, Meyer J. 2004. Complete genomic nucleotide sequence of the temperate bacteriophage Aaφ23 of *Actinobacillus actinomycetemcomitans*. *J Bacteriol* 186:5523–5528. <http://dx.doi.org/10.1128/JB.186.16.5523-5528.2004>.
59. Zhao Y, Wang K, Ackermann H-W, Halden RU, Jiao N, Chen F. 2010. Searching for a “hidden” prophage in a marine bacterium. *Appl Environ Microbiol* 76:589–595. <http://dx.doi.org/10.1128/AEM.01450-09>.
60. Renner T, Specht CD. 2012. Molecular and functional evolution of class I chitinases for plant carnivory in the Caryophyllales. *Mol Biol Evol* 29: 2971–2985. <http://dx.doi.org/10.1093/molbev/mss106>.
61. Ramette A, Frapolli M, Fischer-Le-Saux M, Gruffaz C, Meyer J-M, Défago G, Sutra L, Moëne-Loccoz Y. 2011. *Pseudomonas protegens* sp. nov., widespread plant-protecting bacteria producing the biocontrol compounds 2,4-diacetylphloroglucinol and pyoluteorin. *Syst Appl Microbiol* 34:180–188. <http://dx.doi.org/10.1016/j.sysapm.2010.10.005>.
62. Velesler D, Cambillau C. 2011. A common evolutionary origin for tailed-bacteriophage functional modules and bacterial machineries. *Microbiol Mol Biol Rev* 75:423–433. <http://dx.doi.org/10.1128/MMBR.00014-11>.
63. Loper JE, Hassan KA, Mavrodi DV, Davis EW, Lim CK, Shaffer BT, Elbourne LD, Stockwell VO, Hartney SL, Breakwell K, Henkels MD, Tetu SG, Rangel LI, Kidarsa TA, Wilson NL, van de Mortel JE, Song C, Blumhagen R, Radune D, Hostetler JB. 2012. Comparative genomics of plant-associated *Pseudomonas* spp.: insights into diversity and inheritance of traits involved in multitrophic interactions. *PLoS Genet* 8:e1002784. <http://dx.doi.org/10.1371/journal.pgen.1002784>.
64. Berge O, Monteil CL, Bartoli C, Chandeysson C, Guilbaud C, Sands DC, Morris CE. 2014. A user's guide to a data base of the diversity of *Pseudomonas syringae* and its application to classifying strains in this phylogenetic complex. *PLoS One* 9:e105547. <http://dx.doi.org/10.1371/journal.pone.0105547>.
65. Mavrodi DV, Mavrodi OV, McSpadden-Gardener BB, Landa BB, Weller DM, Thomashow LS. 2002. Identification of differences in genome content among *phlD*-positive *Pseudomonas fluorescens* strains by using PCR-based subtractive hybridization. *Appl Environ Microbiol* 68: 5170–5176. <http://dx.doi.org/10.1128/AEM.68.10.5170-5176.2002>.
66. Garrett CME, Panagopoulos CG, Crosse JE. 1966. Comparison of plant pathogenic *Pseudomonads* from fruit trees. *J Appl Bacteriol* 29:342–356. <http://dx.doi.org/10.1111/j.1365-2672.1966.tb03483.x>.
67. Vidaver AK. 1976. Prospects for control of phytopathogenic bacteria by bacteriophages and bacteriocins. *Annu Rev Phytopathol* 14:451–465. <http://dx.doi.org/10.1146/annurev.py.14.090176.002315>.
68. Yamamoto S, Kasai H, Arnold DL, Jackson RW, Vivian A, Harayama S. 2000. Phylogeny of the genus *Pseudomonas*: intragenomic structure reconstructed from the nucleotide sequences of *gyrB* and *rpoD* genes. *Microbiology* 146:2385–2394.
69. Canchaya C, Proux C, Fournous G, Bruttin A, Brüßow H. 2003. Prophage genomics. *Microbiol Mol Biol Rev* 67:238–276. <http://dx.doi.org/10.1128/MMBR.67.2.238-276.2003>.
70. Martínez-García E, Jatsenko T, Kivisaar M, de Lorenzo V. 2015. Freeing *Pseudomonas putida* KT2440 of its proviral load strengthens endurance to environmental stresses. *Environ Microbiol* 17:76–90. <http://dx.doi.org/10.1111/1462-2920.12492>.
71. Brüßow H, Canchaya C, Hardt W-D. 2004. Phages and the evolution of

- bacterial pathogens: from genomic rearrangements to lysogenic conversion. *Microbiol Mol Biol Rev* 68:560–602. <http://dx.doi.org/10.1128/MMBR.68.3.560-602.2004>.
72. King EO, Ward MK, Raney DE. 1954. Two simple media for the demonstration of pyocyanin and fluorescin. *J Lab Clin Med* 44:301–307.
  73. Bertani G. 1951. Studies on lysogenesis. 1. The mode of phage liberation by lysogenic *Escherichia-coli*. *J Bacteriol* 62:293–300.
  74. Hockett KL, Nishimura MT, Karlsrud E, Dougherty K, Baltrus DA. 2014. *Pseudomonas syringae* CC1557: a highly virulent strain with an unusually small type III effector repertoire that includes a novel effector. *Mol Plant Microbe Interact* 27:923–932. <http://dx.doi.org/10.1094/MPMI-11-13-0354-R>.
  75. Ghequire MG, Li W, Proost P, Loris R, Ghequire MG, Li W, Proost P, Loris R, De Mot R. 2012. Plant lectin-like antibacterial proteins from phytopathogens *Pseudomonas syringae* and *Xanthomonas citri*. *Environ Microbiol Rep* 4:373–380. <http://dx.doi.org/10.1111/j.1758-2229.2012.00331.x>. <http://dx.doi.org/10.1111/j.1758-2229.2012.00331.x>.
  76. Finn RD, Bateman A, Clements J, Coggill P, Eberhardt RY, Eddy SR, Heger A, Hetherington K, Holm L, Mistry J, Sonnhammer EL, Tate J, Punta M. 2014. Pfam: the protein families database. *Nucleic Acids Res* 42:D222–D230. <http://dx.doi.org/10.1093/nar/gkt1223>.
  77. Katoh K, Standley DM. 2013. MAFFT multiple sequence alignment software version 7: improvements in performance and usability. *Mol Biol Evol* 30: 772–780. <http://dx.doi.org/10.1093/molbev/mst010>.
  78. Stamatakis A. 2014. RAXML version 8: a tool for phylogenetic analysis and post-analysis of large phylogenies. *Bioinformatics* 30:1312–1313. <http://dx.doi.org/10.1093/bioinformatics/btu033>.
  79. Abascal F, Zardoya R, Posada D. 2005. ProtTest: selection of best-fit models of protein evolution. *Bioinformatics* 21:2104–2105. <http://dx.doi.org/10.1093/bioinformatics/bti263>.
  80. Bertels F, Silander OK, Pachkov M, Rainey PB, van Nimwegen E. 2014. Automated reconstruction of whole-genome phylogenies from short-sequence reads. *Mol Biol Evol* 31:1077–1088. <http://dx.doi.org/10.1093/molbev/msu088>.
  81. Baltrus DA, Nishimura MT, Romanchuk A, Chang JH, Mukhtar MS, Cherkis K, Roach J, Grant SR, Jones CD, Dangl JL. 2011. Dynamic evolution of pathogenicity revealed by sequencing and comparative genomics of 19 *Pseudomonas syringae* isolates. *PLoS Pathog* 7. <http://dx.doi.org/10.1371/journal.ppat.1002132>.
  82. Arnison PG, Bibb MJ, Bierbaum G, Bowers AA, Bugni TS, Bulaj G, Camarero JA, Campopiano DJ, Challis GL, Clardy J, Cotter PD, Craik DJ, Dawson M, Dittmann E, Donadio S, Dorrestein PC, Entian KD, Fischbach MA, Garavelli JS, Göransson U. 2013. Ribosomally synthesized and post-translationally modified peptide natural products: overview and recommendations for a universal nomenclature. *Nat Prod Rep* 30:108–160. <http://dx.doi.org/10.1039/c2np20085f>.
  83. Farrer RA, Kemen E, Jones JD, Studholme DJ. 2009. *De novo* assembly of the *Pseudomonas syringae* pv. *syringae* B728a genome using Illumina/Solexa short sequence reads. *FEMS Microbiol Lett* 291:103–111. <http://dx.doi.org/10.1111/j.1574-6968.2008.01441.x>.
  84. Ditta G, Stanfield S, Corbin D, Helinski DR. 1980. Broad host range DNA cloning system for gram-negative bacteria: construction of a gene bank of *Rhizobium meliloti*. *Proc Natl Acad Sci U S A* 77:7347–7351. <http://dx.doi.org/10.1073/pnas.77.12.7347>.
  85. Almeida NF, Yan S, Lindeberg M, Studholme DJ, Schneider DJ, Condon B, Liu H, Viana CJ, Warren A, Evans C, Kemen E, Maclean D, Angot A, Martin GB, Jones JD, Collmer A, Setubal JC, Vinatzer BA. 2009. A draft genome sequence of *Pseudomonas syringae* pv. *tomato* T1 reveals a type III effector repertoire significantly divergent from that of *Pseudomonas syringae* pv. *tomato* DC3000. *Mol Plant Microbe Interact* 22:52–62. <http://dx.doi.org/10.1094/MPMI-22-1-0052>.
  86. Buell CR, Joardar V, Lindeberg M, Selengut J, Paulsen IT, Gwinn ML, Dodson RJ, Deboy RT, Durkin AS, Kolonay JF, Madupu R, Daugherty S, Brinkac L, Beanan MJ, Haft DH, Nelson WC, Davidsen T, Zafar N, Zhou L, Liu J. 2003. The complete genome sequence of the Arabidopsis and tomato pathogen *Pseudomonas syringae* pv. *tomato* DC3000. *Proc Natl Acad Sci U S A* 100:10181–10186. <http://dx.doi.org/10.1073/pnas.1731982100>.
  87. Joardar V, Lindeberg M, Jackson RW, Selengut J, Dodson R, Brinkac LM, Daugherty SC, Deboy R, Durkin AS, Giglio MG, Madupu R, Nelson WC, Rosovitz MJ, Sullivan S, Crabtree J, Creasy T, Davidsen T, Haft DH, Zafar N, Zhou L. 2005. Whole-genome sequence analysis of *Pseudomonas syringae* pv. *phaseolicola* 1448A reveals divergence among pathovars in genes involved in virulence and transposition. *J Bacteriol* 187:6488–6498. <http://dx.doi.org/10.1128/JB.187.18.6488-6498.2005>.
  88. Chang JH, Urbach JM, Law TF, Arnold LW, Hu A, Gombar S, Grant SR, Ausubel FM, Dangl JL. 2005. A high-throughput, near-saturating screen for type III effector genes from *Pseudomonas syringae*. *Proc Natl Acad Sci U S A* 102:2549–2554. <http://dx.doi.org/10.1073/pnas.0409660102>.
  89. Baltrus DA, Nishimura MT, Dougherty KM, Biswas S, Mukhtar MS, Vicente J, Holub EB, Dangl JL. 2012. The molecular basis of host specialization in bean pathovars of *Pseudomonas syringae*. *Mol Plant Microbe Interact* 25:877–888. <http://dx.doi.org/10.1094/MPMI-08-11-0218>.
  90. Vinatzer BA, Teitzel GM, Lee M-W, Jelenska J, Hotton S, Fairfax K, Jenrette J, Greenberg JT. 2006. The type III effector repertoire of *Pseudomonas syringae* pv. *syringae* B728a and its role in survival and disease on host and non-host plants. *Mol Microbiol* 62:26–44. <http://dx.doi.org/10.1111/j.1365-2958.2006.05350.x>.